PHYSICAL REVIEW B VOLUME 25, NUMBER 12 15 JUNE 1982

Brillouin instability in n-type piezoelectric semiconductors

P. K. Sen and P. Sen
Department of Physics, Heriot-Watt University, Riccarton, Edinburgh EH14 4AS, United Kingdom
(Received 18 May 1981; revised manuscript received 8 December 1981)

The paper aims at the detailed analytical investigation of Brillouin instability in a magnetoactive n-type cubic piezoelectric semiconducting crystal belonging to class $\bar{4}3m$ under a geometrical configuration which can also be employed in analyzing the phenomenon under either Voigt or Faraday orientation. The electric vector $\vec{E}_0$ of the spatially uniform pump electromagnetic wave (applied along the y axis) is normal to the magnetostatic field $\vec{B}_0$ (along the z axis) as well as to the plane of propagation (x-z plane) of the internally generated low-frequency transverse-acoustic wave $(\omega, \vec{k})$ and the scattered electromagnetic wave $(\omega_1, \vec{k}_1)$. The propagation vectors $\vec{k}$, $\vec{k}_1$ (antiparallel to each other) are in the x-z plane making an angle θ with the x axis. The dispersion relation has been obtained by using a hydrodynamic model of the homogeneous, piezoelectric, one-component (electron) semiconductor plasma, and the critical value of the pump electric field (necessary to achieve physically reasonable growth of an unstable wave) and the growth rate of the unstable Brillouin mode well above the critical field have been obtained for isotropic ($B_0=0$) and magnetoactive ($B_0 \neq 0$) plasmas. We have applied our analysis to a specific semiconductor, n-InSb at 77 K duly irradiated by a pulsed 10.6-μm CO_2 laser for numerical estimation. Qualitative agreement between the analytical results and the numerical analysis has been noticed. The laser wave intensities used here are in the range of 10^9 to 10^{12} $\mathrm{W\,m^{-2}}$ which is assumed to be less than the damage threshold of the InSb crystal. The phase velocity of the growing unstable mode is found to be constant over the whole range of system parameters and equal to the acoustic velocity in the crystal. The magnitude of the critical field decreases with increasing magnetostatic field and decreasing θ. The growth rate increases and attains a maximum value at a certain value of the pump intensity, magnetostatic field, and θ, and if these are raised further, growth rate starts decreasing. The magnitude of the growth rate is found to be $\sim 10^8\ \mathrm{sec^{-1}}$ at laser intensities of the order of $10^{10}\ \mathrm{W\,m^{-2}}$. When the analysis is extended to Voigt and Faraday configurations, the results are not very encouraging.

I. INTRODUCTION

Motivated by the intense interest in the field of stimulated Brillouin scattering (SBS), in the present paper, we have reported the results of the analytical investigations of Brillouin instability in a magnetoactive piezoelectric semiconductor plasma under a general configuration and discussed the possibilities of obtaining maximum growth of the unstable Brillouin mode in the crystal.

Qualitatively, the dielectric constant of a scattering medium depends on some primary excitations in the medium (e.g., molecular vibrations, acoustical and optical phonons) and lead to the coupling of an incident light wave with these excitations. In a semiconductor plasma, the presence of a time varying electric field produces time varying electrostrictive strain in the medium and thus drives an acoustic wave in it; consequently, the phenomenon of SBS occurs due to the interaction of an electromagnetic wave with the generated acoustic wave in the medium. The resultant wave may be scattered at various angles but the scattering maximizes in a backward direction with a characteristic frequency downshift of the acoustic frequency.[1] Accounts of the theory of SBS was given initially by Kroll[2] and Tang[3] and was reviewed by Starunov and Fabelinskii[4] and Fabelinskii.[5] Sen[6] has given a simplified analytical treatment of the SBS phenomena and has analyzed the possibility of Brillouin instability in an n-type transversely magnetoactive piezoelectric semiconductor under a collision-dominated regime neglecting the Doppler shift in the microwave acoustic-frequency range. However, at high electric field amplitudes of the pump wave ($E_0 \sim 10^6$ to $10^7\ \mathrm{V\,m^{-1}}$), the Doppler shift in the acoustic frequency no longer remains negligible and its effect must be incorporated in order to get oneself closer to the physical situation. Asam *et al.*[7] observed SBS in Ge using a pulsed CO_2 laser. Ultrasonic waves in the microwave range duly generated by SBS have been used by Winterling *et al.*[8] to investigate the ultrasonic absorption in quartz at 29 GHz. Sussman and Ridley[9] have reported the Brillouin scattering measurements of amplified acoustic flux in oxygen-doped *n*-GaAs by irradiating the crystal with a cw 1.06-μm Nd—yttrium aluminum garnet (YAG) laser beam. Recently, an experimental observation of SBS in microwave interaction with a plasma has been made by Hue *et al.*[10]

It appears from the available literature that no systematic attempt has been made so far to explore the most appropriate conditions to get maximum amplified acoustic flux in the solid medium using minimum external power. The present authors address themselves to such an attempt by choosing a general configuration of the pump wave, propagation vector, and the magnetostatic field which covers the two important geometries, viz., the Faraday and the Voigt ones as well. We have considered a one-component (electron) cubic piezoelectric semiconducting crystal belonging to class $\bar{4}3m$ subjected to a large transverse magnetostatic field $\vec{B}_0$ in a direction (along z axis) perpendicular to the electric vector $\vec{E}_0$ (along the y axis) of the spatially uniform pump $(\omega_0, \vec{k}_0 0)$ which is propagating in the x-z plane. The scattered electromagnetic and the transverse acoustic waves represented by $(\omega_1, \vec{k}_1)$ and $(\omega, \vec{k})$, respectively, are also propagating in the x-z plane making an angle θ with the x axis. These three waves satisfy the energy and momentum conservation relations yielding $\omega_1 = \omega_0 - \omega$ and $\vec{k}_1 = \vec{k}_0 - \vec{k}$. The investigation can easily be applied individually for Faraday as well as Voigt configurations simply by making $\theta = 90°$ and $0°$, respectively.

The analysis is based on the coupled-mode theory,[11] which was employed earlier by Sen[6] for a simplified treatment of SBS. The incorporation of the finite contributions of the perturbed electron fluid velocity associated with the scattered electromagnetic mode and the effect of Doppler shift on the acoustic frequency adds a new dimension to the analysis presented here.

Nonetheless, the present investigation has been made under the following assumptions: (1) The electric field amplitude of the pump employed in the present investigation has been taken to be less than the damage threshold of the crystal considered. The power density corresponding to the value of the electric field amplitude employed is found to be, quite reasonably, in the range which is normally employed to study the nonlinear optical effects in semiconductors duly irradiated by pulsed laser beams. (2) We have neglected the effects of nonlinear material parameters which play significant roles in strongly piezoelectric semiconductors like $LiNbO_3$ (Ref. 12) by restricting our analysis to moderately piezoelectric semiconductors,[13] viz., III-V binary compounds. (3) The semiconductors have an isotropic and nondegenerate conduction band. (4) The band nonparabolicity which contributes about 3% over the parabolic band structure has been neglected.[13,14] (5) Free-carrier absorption is considered to be negligible (Sec. I of Ref. 6). (6) Dipole approximation is applicable to the pump wave, i.e., the wave vector $\vec{k}_0$ is very small in comparison with $\vec{k}$ and $\vec{k}_1$. (7) We have neglected the thermal effects, because for highly doped semiconductors one can have $\omega_p^2 >> k^2 v_\Theta^2$ (ω_p and v_Θ being the electron plasma frequency and electron thermal velocity, respectively).

Thus, our analysis can be employed effectively in the investigation of SBS in *n*-type heavily doped III-V semiconductors (such as *n*-InSb, *n*-GaAs, etc.) with electron concentrations such that the electron plasma frequencies are large enough and nearly equal to the pump frequency. We have assumed the first-order fluctuations (like $\vec{E}_1$, $\vec{v}_1$, $\vec{J}_1$, n_1, etc.) varying as $\exp[i(\omega t - \vec{k}\cdot\vec{r})]$ and $\exp[i(\omega_1 t - \vec{k}_1\cdot\vec{r})]$ for slow and first components, respectively. The dispersion relations have been solved for complex ω $(=\omega_r + i\omega_i)$ with real positive values of k throughout the present analysis. The propagating mode will be called unstable, growing one only when ω_i is less than 0; $|\omega_i|$ represents the growth rate of the unstable mode. We have made thorough numerical estimations of the entities like the conditions for the onset of instability and growth rate of the unstable Brillouin mode at fields well above the critical pump amplitude necessary to incite the instability in *n*-InSb at 77 K.

The dispersion relation for the scattered modes in a magnetoactive plasma for an arbitrary value of Θ has been formulated in Sec. II. In Sec. III, we have analyzed the results for an isotropic medium $(B_0 = 0)$ and the derived expression for the growth rate of the unstable Brillouin mode has been numerically estimated. Section IV deals with the critical examination of the phenomenon in the magnetoactive medium when the magnetostatic field is such that $\nu < |\omega_c| \leq \omega_p$ (ν and ω_c are the phenomenological electron-collision frequency and electron-cyclotron frequency, respectively). The analytical results obtained under a number of approximations (of course, physically sound) for the growth rate of the unstable mode has been compared with the numerical results obtained by solving the general dispersion relation (which is quartic in complex ω) with the help of a computer over a wide range of magnetostatic field, pump amplitude, and the angle θ. The qualitative agreement between the two approaches has also been shown in the same section. Dispersion relations have further been derived for Voigt and Faraday geometries and analytical expressions for the growth rate and critical value of the pump electric field amplitude have been obtained for both the cases in Sec. V. Section VI is devoted to the important conclusions which can be drawn from the investigations reported in this paper.

II. THEORETICAL FORMULATIONS

We consider the hydrodynamic model of a homogeneous one-component (electron) piezoelectric semiconductor plasma under the geometrical configuration discussed in Sec. I. The time varying electric field amplitude $\vec{E}_0$ of the pump wave produces an electrostrictive strain in the medium which is accompanied by an acoustic wave. This acoustic wave then modulates the optical dielectric constant causing an energy exchange between the electromagnetic waves whose frequencies differ by a small amount equal to the acoustic frequency ω where $\omega << \omega_0$ and consequently, from the frequency matching condition ($\omega_0 = \omega + \omega_1$), one gets $\omega_1 \sim \omega_0$. The net electrostrictive force acting on a unit volume is[1]

$$\vec{F} = \frac{\gamma}{2} \vec{\nabla} E^2 , \tag{2.1}$$

where γ represents the change in optical dielectric constant and is around 10^{-11} F m^{-1}.

We assume that the acoustic wave generated internally is a pure shear wave propagating in the x-z plane with its vibration direction parallel to the y axis. Thus, the acoustic displacement vector $\vec{u}$ can have only two components u_x and u_z. As mentioned in Sec. I, we have chosen a cubic piezoelectric III-V binary semiconducting crystal belonging to class $\bar{4}3m$. When one is concerned with the study of propagation of a low-frequency acoustic vibration in a piezoelectric crystal, the electric and elastic properties of the lattice are coupled and under such circumstance, one must consider the polarization and the electric field accompanying the acoustic vibration. The piezoelectric properties of the material being described by the elements $\underline{e^{ijk}}$ of its piezoelectric tensor.[15] It is well known that the cubic crystals of class $\bar{4}3m$ have only one piezoelectric constant,[16] viz., e_{14} and consequently, the equation of motion of the lattice incorporating the electrostrictive force [given by Eq. (2.1)] and remembering that $u_y = 0$ can be written following Tucker and Rampton[17] and Hayes and Loudon[18] as

$$\rho \frac{\partial^2 u_z}{\partial t^2} = c_{44} \left[\frac{\partial^2 u_x}{\partial z^2} + \frac{\partial^2 u_z}{\partial x \partial z} \right] - e_{14} \frac{\partial E_1}{\partial x} + \frac{\gamma}{2} \frac{\partial}{\partial x} E^2 , \tag{2.2a}$$

and

$$\rho \frac{\partial^2 u_z}{\partial t^2} = c_{44} \left[\frac{\partial^2 u_z}{\partial x^2} + \frac{\partial^2 u_x}{\partial z \partial x} \right] - e_{14} \frac{\partial E_1}{\partial z} + \frac{\gamma}{2} \frac{\partial}{\partial z} E^2 , \tag{2.2b}$$

where ρ is the density of the crystal, c_{44} is the appropriate elastic stiffness constant, and e_{14} is the piezoelectric stress constant. The other basic equations used in the present analysis are

$$\frac{\partial \vec{v}_0}{\partial t} = -\frac{e}{m} (\vec{E}_0 + \vec{v}_0 \times \vec{B}_0) - \nu \vec{v}_0 , \tag{2.3}$$

$$\frac{\partial \vec{v}_1}{\partial t} + (\vec{v}_0 \cdot \vec{\nabla}) \vec{v}_1 = -\frac{e}{m} (\vec{E}_1 + \vec{v}_1 \times \vec{B}_0) - \nu \vec{v}_1 , \tag{2.4}$$

$$\frac{\partial n_1}{\partial t} + (\vec{v}_0 \cdot \vec{\nabla}) n_1 + n_0 (\vec{\nabla} \cdot \vec{v}_1) = 0 , \tag{2.5}$$

and the wave equation[6]

$$\vec{\nabla} \times \vec{\nabla} \times \vec{E}_1 = -\mu_0 \frac{\partial \vec{J}_1}{\partial t} - \frac{1}{c_1^2} \frac{\partial^2 \vec{E}_1}{\partial t^2} + \mu_0 \gamma \frac{\partial^2}{\partial t^2} [(\vec{\nabla} \cdot \vec{u}) \vec{E}_1] . \tag{2.6}$$

Equations (2.3) and (2.4) are the zero and first-order momentum transfer equations in which $\vec{v}_0$ and $\vec{v}_1$ are the oscillatory electron fluid velocities due to the electric field amplitudes of the pump and scattered waves, respectively. Equation (2.5) is the continuity equation in which n_0 and n_1 are the unperturbed and perturbed electron densities, respectively. μ_0 is the absolute permeability, $\vec{J}_1$ represents the perturbed current density, c_1 $[=(\epsilon_0\epsilon_1\mu_0)^{-1/2}]$ is the velocity of light inside the crystal having a dielectric constant ϵ_1, ϵ_0 is the permittivity of free space, and $-e$ and m are the electron charge and effective mass, respectively.

Physically, the high-frequency pump wave generates the low-frequency acoustic wave in the medium and they give rise to the high- and low-frequency components of the carrier density fluctuations (denoted by n_{1f} and n_{1s} and perturbed electron fluid velocities ($\vec{v}_{1f}$ and $\vec{v}_{1s}$) oscillating at frequencies ω_1 $(=\omega_0-\omega)$ and ω of the scattered electromagnetic and acoustic waves, respectively.

To obtain the slow component n_{1s} of the perturbed electron density, we make use of Eqs. (2.2) and the piezoelectric-effect incorporated Poisson equation given by

$$\vec{\nabla}\cdot\vec{E}_1=-\frac{n_1 e}{\epsilon}-\frac{e_{14}}{\epsilon}\left[\frac{\partial^2 u_x}{\partial x^2}+\frac{\partial^2 u_z}{\partial z^2}\right], \tag{2.7}$$

and consequently, one finds

$$n_{1s}=\frac{\epsilon}{e}\left[\frac{\left[\omega^2-k^2c_t^2-\frac{e_{14}e'_{14}}{\rho\epsilon}k^2\right]}{(\omega^2-k^2c_t^2)}\right]\left[\frac{\partial E_{1x}}{\partial x}+\frac{\partial E_{1z}}{\partial z}\right], \tag{2.8}$$

where $c_t=(c_{44}/\rho)^{1/2}$ and is the transverse acoustic velocity in the crystal and $e'_{14}=e_{14}-\gamma E_0/2$, $\epsilon=\epsilon_0\epsilon_\lambda$. In obtaining the above equation, we have neglected $\partial^2 u_x/\partial z\partial x$ and $\partial^2 u_z/\partial x\partial z$ in comparison with $\partial^2 u_z/\partial x^2$ and $\partial^2 u_x/\partial z^2$, respectively, in Eqs. (2.2) which makes the analysis much simpler without any significant loss of generality.

The fast component n_{1f} can be expressed in terms of n_{1s} by using Eqs. (2.3)–(2.5) and (2.7) as

$$n_{1f}=-\frac{4ik_x\omega_c v_{0y}\delta}{\omega_0(\nu^2+\delta^2)}n_{1s}, \tag{2.9}$$

where $\delta=\omega_0-\omega_p$, $\omega_p=n_0e^2/m\epsilon$, and $\omega_c=-eB_0/m$. In deriving Eq. (2.9), we have restricted ourselves to the range $\omega_p\sim\omega_0$ and followed the usual procedure.[19] The two components of the zero-order oscillatory electron fluid velocity, viz., v_{0x} and v_{0y} are obtained from Eq. (2.3) as

$$v_{0x}=-\frac{eE_0}{m}\frac{\omega_c}{\omega_c^2+(i\omega_0+\nu)^2}, \tag{2.10a}$$

and

$$v_{0y}=-\frac{eE_0}{m}\frac{(i\omega_0+\nu)}{\omega_c^2+(i\omega_0+\nu)^2}. \tag{2.10b}$$

Similarly, the components of $\vec{v}_1$ $(=\vec{v}_{1f}+\vec{v}_{1s})$ are derived from Eq. (2.4) and given by

$$v_{1x}=-\frac{e}{m}\sum_{q=s,f}\frac{\omega_q E_{1x}+\omega_c E_{1y}}{\omega_c^2+\omega_q^2}, \tag{2.11a}$$

$$v_{1y}=-\frac{e}{m}\sum_{q=s,f}\left[-\frac{\omega_c}{\omega_c^2+\omega_q^2}E_{1x}+\left[\frac{1}{\omega_q}-\frac{\omega_c^2}{\omega_q(\omega_c^2+\omega_q^2)}\right]E_{1y}\right], \tag{2.11b}$$

and

$$v_{12}=-\frac{e}{m}\sum_{q=s,f}\frac{1}{\omega_q}E_{1z}, \tag{2.11c}$$

where $\omega_s=i(\omega-k_xv_{0x})+\nu$ and $\omega_f=i(\omega_1-k_xv_{0x})+\nu$. The perturbed electron current density is given by

$$\vec{J}_1=-en_0(\vec{v}_{1f}+\vec{v}_{1s})-e\vec{v}_0(n_{1f}+n_{1s}). \tag{2.12}$$

One finds the components of $\vec{J}_1$ along the three axes by using Eqs. (2.8) to (2.12) as

$$J_{1x}=\left[\omega_p^2\epsilon\left[\frac{\omega_s}{\omega_c^2+\omega_s^2}+\frac{\omega_f}{\omega_c^2+\omega_f^2}\right]+\frac{i\epsilon k_xv_{0x}X}{2(\omega^2-k^2c_t^2)}\left[\omega^2-k^2c_t^2-\frac{e_{14}e'_{14}}{\rho\epsilon}k^2\right]\right]E_{1x}$$

$$+\omega_c\omega_p^2\epsilon\left[\frac{1}{\omega_c^2+\omega_s^2}+\frac{1}{\omega_c^2+\omega_f^2}\right]E_{1y}+\frac{i\epsilon k_2v_{0y}X}{2(\omega^2-k^2c_t^2)}\left[\omega^2-k^2c_t^2\frac{e_{14}e'_{14}k^2}{\rho\epsilon}\right]E_{1z}, \tag{2.13a}$$

$$J_{1y}=\left[\frac{i\epsilon k_x v_{0y}X}{2(\omega^2-k^2c_t^2)}\left[\omega^2-k^2c_t^2-\frac{e_{14}e'_{14}k^2}{\rho\epsilon}\right]-\omega_c\omega_p^2\epsilon\left[\frac{1}{\omega_c^2+\omega_s^2}+\frac{1}{\omega_c^2+\omega_f^2}\right]\right]E_{1x}$$

$$+\omega_p^2\epsilon\left[\frac{1}{\omega_s}+\frac{1}{\omega_f}-\frac{\omega_c^2}{\omega_s(\omega_c^2+\omega_s^2)}-\frac{\omega_c^2}{\omega_f(\omega_c^2+\omega_f^2)}\right]E_{1y}+\frac{i\epsilon k_z v_{0y}X}{2(\omega^2-k^2c_t^2)}\left[\omega^2-k^2c_t^2-\frac{e_{14}e'_{14}k^2}{\rho\epsilon}\right]E_{1z}\,, \tag{2.13b}$$

and

$$J_{1z}=\omega_p^2\epsilon(1/\omega_s+1/\omega_f)E_{1z}\,, \tag{2.13c}$$

where

$$X=1-4ik_x v_{0y}\omega_c\delta/[\omega_0(\nu^2+\delta^2)]\,.$$

Using the wave equation (2.6) and substituting the components of $\vec{J}_1$ from Eqs. (2.13) therein, one can get the general dispersion relation as

$$\begin{vmatrix} a_{11} & a_{12} & a_{13} \\ a_{21} & a_{22} & a_{23} \\ a_{31} & 0 & a_{33} \end{vmatrix}=0\,, \tag{2.14}$$

where

$$a_{11}=-k_z^2-\frac{\omega_1^2}{c_1^2}-\frac{\mu_0\gamma\omega_1^2e'_{14}E_0k_x^2}{\rho(\omega^2-k^2c_t^2)}+\frac{i\omega_1\omega_p^2}{c_1^2}\left[\frac{\omega_s}{\omega_c^2+\omega_s^2}+\frac{\omega_f}{\omega_c^2+\omega_f^2}\right]-\frac{k_x v_{0x}\omega_1 X}{2c_1^2(\omega^2-k^2c_t^2)}\left[\omega^2-k^2c_t^2-\frac{e_{14}e'_{14}k^2}{\rho\epsilon}\right],$$

$$a_{12}=\frac{i\omega_1\omega_p^2\omega_c}{c_1^2}\left[\frac{1}{\omega_c^2+\omega_s^2}+\frac{1}{\omega_c^2+\omega_f^2}\right],$$

$$a_{13}=k_xk_z-\frac{k_x v_{0x}\omega_1 X}{2c_1^2(\omega^2-k^2c_t^2)}\left[\omega^2-k^2c_t^2-\frac{e_{14}e'_{14}k^2}{\rho\epsilon}\right],$$

$$a_{21}=-\frac{k_x v_{0x}\omega_1 X}{2c_1^2(\omega^2-k^2c_t^2)}\left[\omega^2-k^2c_t^2-\frac{e_{14}e'_{14}k^2}{\rho\epsilon}\right]-\frac{i\omega_p^2\omega_c\omega_1}{c_1^2}\left[\frac{1}{\omega_c^2+\omega_s^2}+\frac{1}{\omega_c^2+\omega_f^2}\right],$$

$$a_{22}=-k_x^2-k_z^2-\frac{\omega_1^2}{c_1^2}+\frac{i\omega_p^2\omega_1}{c_1^2}\left[\frac{1}{\omega_s}+\frac{1}{\omega_f}-\frac{\omega_c^2}{\omega_s(\omega_c^2+\omega_s^2)}-\frac{\omega_c^2}{\omega_f(\omega_c^2+\omega_f^2)}\right],$$

$$a_{23}=-\frac{\omega_1 k_z v_{0y}X}{2c_1^2(\omega^2-k^2c_t^2)}\left[\omega^2-k^2c_t^2-\frac{e_{14}e'_{14}k^2}{\rho\epsilon}\right],$$

$$a_{31}=k_xk_z\,,$$

and

$$a_{33}=-k_x^2-\frac{\omega_1^2}{c_1^2}-\frac{\mu_0\gamma\omega_1^2e'_{14}E_0k_z^2}{\rho(\omega^2-k^2c_t^2)}+\frac{i\omega_1\omega_p^2}{c_1^2}(1/\omega_s+1/\omega_f)\,.$$

The linear representation of the dispersion relation is

$$a_{22}(a_{11}a_{33}-a_{13}a_{31})=a_{12}(a_{21}a_{33}-a_{23}a_{31})\,. \tag{2.15}$$

From the knowledge of the different physical parameters for the semiconductors like n-GaAs and n-InSb, one can notice that $a_{11} >> a_{12}$ but a_{21} is comparable to a_{22} for the finite values of both k_x and k_z. Thus, a_{12} can be neglected and the dispersion relation reduces to a simpler form

$$a_{11}a_{33}=a_{13}a_{31} \; . \tag{2.16}$$

The substitution of the values of $a_{11}, a_{13}, a_{31}, a_{33}$ yields the following dispersion relation after some mathematical simplification:

$$\begin{aligned}
&(\omega^2-k^2c_t^2)^2\Bigg\{\Bigg[-k_z^2-\frac{\omega_1^2}{c_1^2}+\frac{i\omega_1\omega_p^2}{c_1^2}\Bigg[\frac{\omega_s}{\omega_c^2+\omega_s^2}+\frac{\omega_f}{\omega_c^2+\omega_f^2}\Bigg]\Bigg]\Bigg[-k_x^2-\frac{\omega_1^2}{c_1^2}+\frac{i\omega_1\omega_p^2}{c_1^2}\Bigg[\frac{1}{\omega_s}+\frac{1}{\omega_f}\Bigg]\Bigg]-k_x^2k_z^2\Bigg\}\\
&\quad+(\omega^2-k^2c_t^2)\Bigg[\Bigg\{\frac{\mu_0\gamma\omega_1^2e'_{14}E_0k_z^2}{\rho}\Bigg[-k_z^2-\frac{\omega_1^2}{c_1^2}+\frac{i\omega_1\omega_p^2}{c_1^2}\Bigg[\frac{\omega_s}{\omega_c^2+\omega_s^2}+\frac{\omega_f}{\omega_c^2+\omega_f^2}\Bigg]\Bigg]\Bigg\}\\
&\quad-\Bigg[\frac{\mu_0\gamma\omega_1^2e'_{14}E_0k_x^2}{\rho}+\frac{k_xv_{0x}\omega_1X}{2c_1^2}\Bigg[\omega^2-k^2c_t^2-\frac{e_{14}e'_{14}k^2}{\rho\epsilon}\Bigg]\Bigg]\\
&\quad\times\Bigg[-k_x^2-\frac{\omega_1^2}{c_1^2}+\frac{i\omega_1\omega_p^2}{c_1^2}\Bigg[\frac{1}{\omega_s}+\frac{1}{\omega_f}\Bigg]\Bigg]-\frac{k_xv_{0x}\omega_1Xk_z^2}{2c_1^2}\Bigg[\omega^2-k^2c_t^2-\frac{e_{14}e'_{14}k^2}{\rho\epsilon}\Bigg]\Bigg]\\
&\quad=\frac{\mu_0\gamma\omega_1^2e'_{14}E_0k_z^2}{\rho}\Bigg[\frac{\mu_0\gamma\omega_1^2e'_{14}E_0k_x^2}{\rho}+\frac{k_xv_{0x}\omega_1X}{2c_1^2}\Bigg[\omega^2-k^2c_t^2-\frac{e_{14}e'_{14}k^2}{\rho\epsilon}\Bigg]\Bigg] .
\end{aligned} \tag{2.17}$$

Equation (2.17) can be used to investigate the possibility of Brillouin instability in a dense ($\omega_p \sim \omega_0$), isotropic as well as magnetoactive ($\omega_c \sim \omega_p$), cubic piezoelectric semiconductor plasma over a wide range of system parameters with $\omega < \nu$, $\omega = \nu$, and $\omega > \nu$, provided that the other assumptions mentioned in Sec. I are correct.

III. ISOTROPIC SEMICONDUCTOR PLASMA

In an isotropic plasma with $B_0=0$, the dispersion relation (2.17) reduces to the following form:

$$\begin{aligned}
&(\omega^2-k^2c_t^2)\Bigg[\Bigg[-k_z^2-\frac{\omega_1^2}{c_1^2}+\frac{i\omega_1\omega_p^2}{c_1^2\nu}\Bigg]\Bigg[-k_x^2-\frac{\omega_1^2}{c_1^2}+\frac{i\omega_1\omega_p^2}{c_1^2\nu}\Bigg]+k_x^2k_z^2\Bigg]\\
&\qquad+\frac{\mu_0\gamma\omega_1^2e'_{14}E_0}{\rho}\Bigg[k_z^2\Bigg[-k_z^2-\frac{\omega_1^2}{c_1^2}+\frac{i\omega_1\omega_p^2}{c_1^2\nu}\Bigg]-k_x^2\Bigg[-k_x^2-\frac{\omega_1^2}{c_1^2}+\frac{i\omega_1\omega_p^2}{c_1^2\nu}\Bigg]\Bigg]=0 \; .
\end{aligned} \tag{3.1}$$

The above equation describes Brillouin instability in a two-dimensional case with both k_x and k_z being finite.

It can be observed from the above equation that the acoustic and the electromagnetic modes (obtainable by equating to zero the first and the second factor, respectively, in the left-hand side) are coupled via the nonlinear force due to electrostriction in the piezoelectric semiconductor. The presence of the high-frequency pump with $E_0 \neq 0$ is a precondition for the coupling (as is evident from the same equation). Since we have assumed spatially uniform pump with $k_0 << k$, one can easily take k_x^2, $k_z^2 >> \omega_1^2/c_1^2$ for $0° < \theta < 90°$

as $\omega_1^2/c_1^2 \sim k_0^2$ with $\omega_1 \sim \omega_0$. Using this approximation, after algebraic simplifications, Eq. (3.1) yields

$$(\omega^2-k^2c_t^2)\left[k^2-\frac{i\omega_0\omega_p^2}{c_1^2\nu}\right]=\frac{i\mu_0\gamma c_t^2\nu\omega_0 e'_{14}E_0}{\rho\omega_p^2}\left[-(k_x^4+k_z^4)+\frac{i\omega_0\omega_p^2k^2}{c_1^2\nu}\right]. \tag{3.2}$$

To explore the possibility of instability, we solve the dispersion relation for complex $\omega(=\omega_r+i\omega_i)$ with real positive values of the wave number k such that $\omega_r=kc_t$. Equating the imaginary parts, one can have

$$\omega_i=-\frac{\mu_0\gamma\omega_0 e'_{14}c_1^2\nu k E_0}{2\omega_p^2\rho c_t}\left[1-\frac{2k_x^2k_z^2}{\left[k^4+\frac{\omega_0^2\omega_p^4}{\nu^2c_1^4}\right]}\right]. \tag{3.3}$$

Equation (3.3) yields $\omega_i<0$ because the factor within the square brackets is always positive. This relation gives a zero threshold value of the pump electric field amplitude and for a real semiconductor as shown below, the results are not very encouraging.

The numerical calculations of growth rate $|\omega_i|$ of the unstable Brillouin mode for n-InSb at 77 K duly irradiated by a pulsed 10.6-μm CO_2 laser ($\omega_0 \sim 1.78\times10^{14}$ sec^{-1}) is made with $k=2\times10^7$ m^{-1}, $\nu=3.5\times10^{11}$ sec^{-1}, and $\omega_p=1.775\times10^{14}$ sec^{-1}. The other physical constants are: $m=0.0138m_0$, $e_{14}=0.054$ C m^{-2}, $\rho=5.8\times10^3$ kg m^{-3}, $\epsilon_\lambda=17.8$, and remembering that the ratio between transverse and longitudinal sound velocities varies from 0 to $1/\sqrt{2}$, we have taken $c_t=1/\sqrt{2}\times4\times10^3$ m sec^{-1}. Using these values in Eq. (3.3), one obtains $|\omega_i|\sim8.26\times10^{-6}(E_0)$ which yields a very low value of the growth rate even at a moderately high value of E_0. Practically, one can say that no growing unstable Brillouin mode would be observed in isotropic crystal at pump intensity less than that which can cause damage to the crystal under the configuration when the pump amplitude is normal to the direction of propagation of the scattered wave, i.e., when $\vec{E}_0$ is perpendicular to $\vec{k}$. This result is different from that obtained by Sen[6] who found a moderate growth of the unstable mode in the same crystal with $\vec{E}_0$ being parallel to $\vec{k}$ and $B_0=0$.

IV. MAGNETOACTIVE PLASMA

The general dispersion relation (2.17) derived in Sec. II has been solved under a number of physically sound approximations in Sec. IV A and an expression for the growth rate has been obtained in order to study the qualitative nature of the phenomenon of Brillouin instability in a magnetized crystal. The results of the computer analysis of the relation (2.17) is presented in Sec. IV B describing more accurately and elaborately the dependence of growth rate of the unstable mode on the different physical parameters. An effort has been made to establish a clarity between the two approaches in Sec. IV C.

A. Analytical approach

We have considered the range of θ inbetween 0° and 90° (e.g., from 5° to 85°). The cases at $\theta=0°$ and 90° have been discussed in Sec. V. We take $\omega_p\sim\omega_1\sim\omega_0$ and $\omega_0>>\nu$, k_xv_{0x},ω; $\nu<<|\omega_c|$ and $|\omega_c|<\omega_0$. They result into the following simplifications:

$$\left[\frac{\omega_s}{\omega_c^2+\omega_s^2}+\frac{\omega_f}{\omega_c^2+\omega_f^2}\right]\sim\frac{\omega_0}{\omega_0^2-\omega_c^2},$$

$$(1/\omega_s+1/\omega_f)\sim1/\omega_s,$$

and

$$k_x^2\omega_0/(\omega_0^2-\omega_c^2)<<k_z^2/(\nu-ik_xv_{0x}).$$

Using these mathematical approximations, the dispersion relation (2.17) can be reduced to

$$(\omega^2-k^2c_t^2)\left[\left[-k_z^2+\frac{\omega_0\omega_p^2}{c_1^2(\omega_0^2-\omega_c^2)}\right]\left[-k_x^2+\frac{i\omega_0\omega_p^2}{c_1^2(\nu-ik_xv_{0x})}\right]+k_x^2k_z^2\right]$$

$$=-\frac{\mu_0\gamma\omega_0^2e'_{14}k_z^2E_0}{\rho}\left[-k_z^2+\frac{\omega_0\omega_p^2}{c_1^2(\omega_0^2-\omega_c^2)}\right]-\frac{k_xv_{0x}\omega_0e_{14}e'_{14}X}{2c_1^2\rho\epsilon}\left[k_x^4+k_z^4-\frac{i\omega_0\omega_p^2k_x^2}{c_1^2(\nu-ik_xv_{0x})}\right]. \tag{4.1}$$

Equation (4.1) shows that the acoustic mode and the scattered electromagnetic mode are coupled via the pump electric field. Moreover, at finite value of the pump amplitude, the coupling is possible in both piezoelectric as well as the semiconductors exhibiting the properties of electrostriction remembering that $e'_{14}=e_{14}-\gamma E_0/2$. It can further be noticed from a rough numerical estimation for any piezoelectric semiconductor that the piezoelectric coupling is much stronger than the electrostrictive coupling.

We now proceed to investigate the possibility of Brillouin instability. We separate the real and imaginary parts on the two sides of Eq. (4.1); the imaginary parts yield the expression for ω_i as

$$\omega_i=\frac{c_1^2(\nu^2+k_x^2v_{0x}^2)}{2\omega_p^2\nu k c_1 k_z^2}\left[\frac{\mu_0\gamma\omega_0 e'_{14}k_z^2E_0}{\rho}+\frac{k_x v_{0x}e_{14}e'_{14}X}{2c_1^2\rho\epsilon}\left[k_x^4+k_z^4+\frac{\omega_0\omega_p^2k_x^3v_{0x}}{c_1^2(\nu^2+k^2v_{0x}^2)}\right]\right] . \tag{4.2}$$

In obtaining the above equation, only the numerically dominant terms have been taken into account. At $\omega_c=0$, the results agree with those predicted in Sec. III. It is apparent from the above expression that at $E_0=0$, $\omega_i=0$, which means that the instability is having a zero threshold. However, as long as the magnetostatic field remains considerably low, one achieves a negligible growth of the scattered modes. A numerical estimation shows that the second term within the square brackets in Eq. (4.2) becomes dominant as compared to the first one only when $|\omega_c|>10^{12}$ sec^{-1}. As is mentioned earlier in this section that the phenomenon has been studied at $|\omega_c|>>\nu$, we neglect the first term and thus obtain an expression for ω_i as

$$\omega_i=-\frac{e_{14}e'_{14}\omega_c\nu e k_x E_0}{4k_z^2kc_t m\epsilon\rho\omega_p^2(\omega_0^2-\omega_c^2)}\left[1+\frac{k_x v_{0x}\delta}{(\nu^2+4\delta^2)}\right]$$
$$\times\left[k_x^4+k_z^4+\frac{\omega_0\omega_p^2k_x^3v_{0x}}{c_1^2(\nu^2+k_x^2v_{0x}^2)}\right] , \tag{4.3}$$

where we have substituted the value of X from Sec. II. Remembering that ω_c is having a negative value (as it is defined by $-eB_0/m$), the growth of the unstable mode can be possible only when

$$\left[1+\frac{k_x v_{0x}\delta}{(\nu^2+4\delta^2)}\right]<0 ,$$

provided that

$$(k_x^4+k_z^4)+\omega_0\omega_p^2k_x^3v_{0x}/[c_1^2(\nu^2+k_x^2v_{0x}^2)]$$

is positive which is valid for the values of $E_0>2\times10^5$ V m^{-1}. Thus we see that the condition of obtaining a significant growth rate is dependent on electric field amplitude of the pump wave and it should have a value such that the above condition is satisfied. We denote this electric field amplitude above which one can expect a considerable growth of the unstable mode by $E_{\rm cr}$ (the subscript cr stands for critical) and its value is given by

$$E_{\rm cr}=\frac{m(\omega_0^2-\omega_c^2)(\nu^2+4\delta^2)}{4ek_x|\omega_c|\delta} . \tag{4.4}$$

It is worth mentioning at this juncture that the factor $(\omega_0^2-\omega_c^2)$ should be replaced by $\{-[(i\omega_0+\nu)^2+\omega_c^2]\}$, if one wants to study the phenomena at $\omega_0\approx\omega_c$.

At low values of E_0 ($\sim5\times10^5$ V m^{-1}), the factor $1+k_x v_{0x}\delta/(\nu^2+4\delta^2)$ remains positive and the condition of instability is then determined by

$$\frac{\omega_0\omega_p^2k_x^2v_{0x}}{c_1^2\nu^2}>(k_x^4+k_z^4) ,$$

or

$$E_0>\frac{mc_1^2\nu^2(\omega_0^2-\omega_c^2)}{e|\omega_c|\omega_0\omega_p^2k_x^3}(k_x^4+k_z^4) . \tag{4.5}$$

It should be noted here that all these conditions have been derived for $|\omega_c|<\omega_0$ range of magnetostatic field, i.e., $(\omega_0^2-\omega_c^2)$ was assumed to be positive. We have not made any attempt to find out the conditions of instability above this range because the cyclotron absorption and Landau damping may become important in such a high range of applied magnetostatic field and the present analysis does not take into account these effects.

B. Computer analysis

For this purpose, we have solved Eq. (2.17) with no further approximation except that $c_t^2>>e_{14}e'_{14}/\rho\epsilon$. We have written Eq. (2.17) in the form

$$\omega^4\left[-2k_x^2k_z^2-\frac{k^2k_xv_{0x}X}{2c_1^2}+i\frac{\omega_0\omega_p^2k_z^2}{\omega_sc_1^2}\right]$$
$$+\omega^2\left[4k^2c_1^2k_x^2k_z^2+\frac{k_xv_{0x}\omega_0c_1^2X}{2c_1^2}(k^4+k_x^4+k_z^4)-\frac{\mu_0\gamma e'_{14}E_0\omega_0^2(k_x^4+k_z^4)}{\rho}-\frac{k_z^2k_xv_{0x}\omega_0\gamma e_{14}E_0X}{2\rho\epsilon c_1^4}+\frac{i\omega_0\omega_p^2k_2^2}{\omega_sc_1^2}\right]$$
$$+k^2c_t^2\omega_0(k_x^4+k_z^4)\left[\frac{\mu_0\gamma e'_{14}\omega_0E_0}{\rho}-\frac{k_xv_{0x}c_t^2X}{2c_1^2}\right]-2k^4c_t^4k_x^2k_z^2+\frac{\mu_0\gamma\omega_0^3e'_{14}E_0k_x^2k_z^2}{\rho}\left[\frac{k_xv_{0x}c_t^2X}{2c_1^2}-\frac{\mu_0\gamma\omega_0e'_{14}E_0}{\rho}\right]$$
$$+\frac{i\omega_0\omega_p^2k_2^2k^4c_1^4}{\omega_sc_1^2}=0\;. \tag{4.6}$$

The above equation is quartic in ω and has been solved for a real positive value of k $(=2\times10^7\ \mathrm{m}^{-1})$. The solutions for complex ω $(=\omega_r+i\omega_i)$ with $\omega_i<0$ have been considered as solutions representing the unstable Brillouin mode propagating with a phase velocity $v_\phi(=\omega_r/k)$ and a growth rate $|\omega_i|$. The analysis is made for $\theta=15°$ to $75°$, $|\omega_c|=5\times10^{13}$ to $1.7\times10^{14}\ \mathrm{sec}^{-1}$, and $E_0=10^6$ to $1.5\times10^7\ \mathrm{V\,m}^{-1}$. The crystal considered for this purpose is n-InSb at 77 K duly irradiated by a pulsed 10.6 μm CO_2 laser. The material parameters chosen are already mentioned in Sec. III.

The results are plotted in Fig. 1–3. Figure 1 shows the variation of the growth rate $|\omega_i|$ with electric field amplitude of the pump E_0. The maximum value of $|\omega_i|$ occurs at $E_0\sim1.1\times10^7\ \mathrm{V\,m}^{-1}$, $\theta=60°$, and $|\omega_c|=1.5\times10^{14}\ \mathrm{sec}^{-1}$. A further increase in E_0 reduces the growth rate of the unstable mode. However, we have limited our-

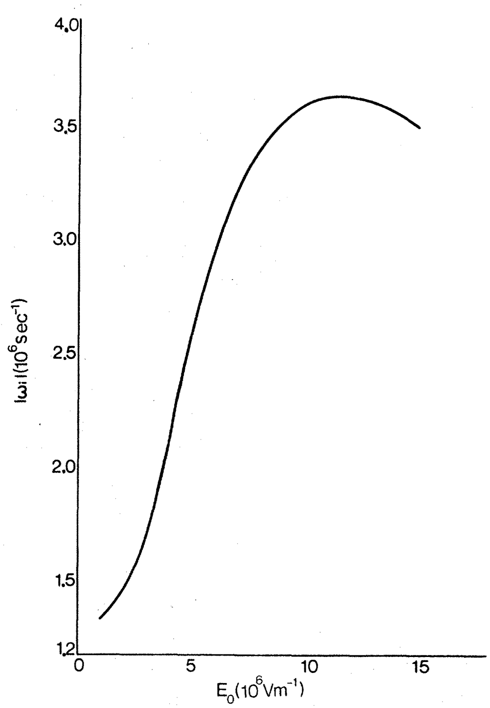

FIG. 1. Dependence of growth rate $|\omega_i|$ of the unstable Brillouin mode on the pump electric field amplitude E_0 at $\theta=60°$ and $|\omega_c|=1.5\times10^{14}\ \mathrm{sec}^{-1}$.

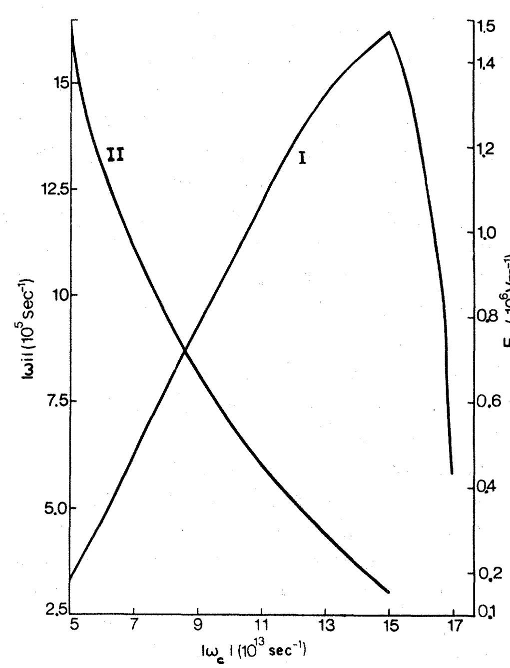

FIG. 2. Dependence of growth rate $|\omega_i|$ on the magnetostatic field (in terms of $|\omega_c|$) at $\theta=30°$ and pump field $E_0=5\times10^6\ \mathrm{V\,m}^{-1}$ (represented by curve I); Variation of the critical pump amplitude E_{cr} with $|\omega_c|$ at $\theta=30°$ (represented by curve II).

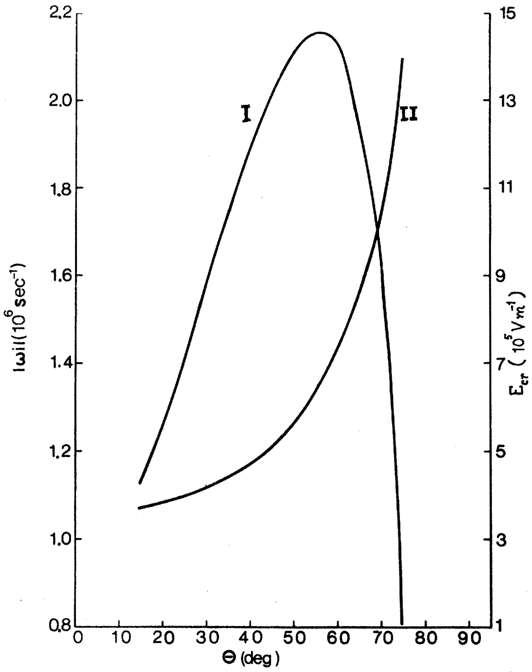

FIG. 3. Dependence of growth rate $|\omega_i|$ on the angle θ at $E_0=9\times10^6$ V m^{-1} and $|\omega_c|=1.1\times10^{14}$ sec^{-1} (curve I); variation of E_{cr} with θ at $|\omega_c|=1.1\times10^{14}$ sec^{-1} (curve II).

selves to a highest value of E_0 of the order of 1.5×10^7 V m^{-1}, as there is a possibility of damage to the crystal if a very high-intensity laser beam with $E_0>1.5\times10^7$ V m^{-1} is applied. The nature of dependence of $|\omega_i|$ as well as E_{cr} on magnetic field are plotted in Fig. 2 where curve I shows the variation of growth rate with applied magnetostatic field (in terms of $|\omega_c|$) and curve II represents the variation of E_{cr} with $|\omega_c|$. Curve I indicates that the growth rate of the unstable Brillouin mode increases rapidly with increase in $|\omega_c|$ up to a value of $|\omega_c|\sim1.5\times10^{14}$ sec^{-1}. A further rise in $|\omega_c|$ causes a sharp fall in $|\omega_i|$. Curve II is plotted for a fixed value of θ ($=30°$ in this case). One can notice that E_{cr} decreases as $|\omega_c|$ is increased. Figure 3 deals with the relation between $|\omega_i|$ and θ (curve I) and E_{cr} and θ (curve II). From the nature of curve I, one can conclude that the role of θ in obtaining considerable growth of the unstable mode is critical for the reason that at lower values of θ (i.e., $\theta\lesssim60°$), $|\omega_i|$ increases with the increase in θ with the maxima being obtainable at $\theta\sim60°$ but after that $|\omega_i|$ decreases very rapidly with increasing θ and for $\theta\sim90°$, $|\omega_i|$ becomes almost vanishingly small. From curve II, we can infer that the critical pump field becomes higher at larger value of θ and for $\theta\sim90°$, it is appreciably large and may be even higher than the damage threshold of the crystal. Thus, Fig. 3 indicates that θ should be around 60° in order to achieve a large growth of the unstable mode without causing any damage to the crystal. It is worth mentioning here that the value of θ at which one can get maximum growth rate is dependent on the values of E_0 and $|\omega_c|$ chosen for the geometry.

While watching the nature of dependence of the phase velocity $v_\phi(=\omega_r/k)$ of the unstable Brillouin mode on the different system parameters like the electric field amplitude of the pump, magnetostatic field, and the angle θ, we have noticed that it remains fairly constant over the whole range of these parameters and its magnitude is exactly equal to the acoustic velocity inside the crystal (viz., $v_\phi\approx c_t\sim2.83\times10^3$ m sec^{-1} in n-InSb crystal).

C. Comparison between the two approaches

Here, we have addressed ourselves to the question of establishing a relationship between the results discussed in the above two subsections. Let us first take the case of the behavior of the critical pump amplitude E_{cr} below which the unstable mode does not exhibit any significant growth. From Eq. (4.4) we notice that E_{cr} decreases as $|\omega_c|$ is increased when $|\omega_c|<\omega_0$. A look at curve II of Fig. 2 agrees well with this behavior for $|\omega_c|<\omega_0$. If considered the nature of dependence of E_{cr} on θ, the same equation (4.4) manifests that E_{cr} will be higher at higher values of θ as k_x decreases with increase in θ and E_{cr} rises very sharply as θ tends to 90° and theoretically, E_{cr} tends to infinity as θ approaches 90°. If we compare this result with curve II of Fig. 3, we again achieve a fairly good agreement between the two approaches. Now we examine the agreement in relation to the growth rate $|\omega_i|$. From Eq. (4.3) one can notice that the analytical expression for $|\omega_i|$ is too complicated to handle for obtaining a simple relation between $|\omega_i|$ and any of the parameters like E_0, $|\omega_c|$, and θ. Of course, to find out the possibilities of existence of maximas of $|\omega_i|$ with respect to E_0, $|\omega_c|$, and θ, we have derived $\partial|\omega_i|/\partial E_0$, $\partial|\omega_i|/\partial|\omega_c|$, and $\partial|\omega_i|/\partial\theta$ by assigning constant values to the remaining variables (e.g., $|\omega_c|$ and θ in the first case) and equated them individually to zero. The value of E_0 obtained from $\partial|\omega_i|/\partial E_0=0$ corresponds to the maximum growth rate. Likewise, the expressions can be obtained to find out the maximas of $|\omega_i|$ corresponding to $|\omega_c|$ and θ. Figure 1 as well as curve I in Fig. 2 and 3 exhibit the same nature of dependence. However, the qualitative agreement between the two approaches obtained is not exact in these cases.

V. VOIGT AND FARADAY GEOMETRIES

The general dispersion relation represented by Eq. (2.17) no longer remains valid for these two cases. Thus, under these geometrical configurations, one must address oneself to the relation (2.15) and proceed as follows: A simple look at Eq. (2.15) shows that the coefficient a_{31} becomes zero when either k_x or k_z is equal to zero. Consequently, Eq. (2.15) reduces to

$$a_{33}(a_{22}a_{11}-a_{12}a_{21})=0 \ . \qquad (5.1)$$

A. Voigt geometry ($k_z=0$, $k_x\neq 0$)

Equation (5.1) leads to

$$a_{33}=0$$

or

$$a_{22}a_{11}-a_{12}a_{21}=0 \ . \qquad (5.2)$$

$a_{33}=0$ gives

$$k_x^2+\frac{\omega_1^2}{c_1^2}-i\frac{\omega_1\omega_p^2}{c_1^2}(1/\omega_s+1/\omega_f)=0 \ ,$$

which merely represents the dispersion relation for a single electromagnetic mode propagating along x axis. This mode is of no importance under the present context as we are solely concerned with the scattering of the electromagnetic wave due to the internally generated acoustic wave in the medium. However, Eq. (5.2) yields

$$(\omega^2-k^2c_t^2)\left[1+\frac{\omega_p^2}{(\omega_c^2-\omega_0^2)}+\frac{kv_{0x}X}{2\omega_0}\right] = -\frac{\gamma e'_{14}E_0k^2}{\rho\epsilon}+\frac{k^3v_{0x}e_{14}e'_{14}X}{2\omega_0\rho\epsilon} + \frac{ikv_{0x}e_{14}e'_{14}\omega_p^2\omega_cX}{2c_1^2\rho\epsilon(\omega_c^2-\omega_0^2)} \ , \qquad (5.3)$$

where k stands for k_x. Here, we have assumed that

$$\frac{\omega_s}{\omega_c^2+\omega_s^2}+\frac{\omega_f}{\omega_c^2+\omega_f^2}\sim\frac{\omega_f}{\omega_c^2+\omega_f^2} \ .$$

Equation (5.3) shows that the acoustic and the electromagnetic modes are coupled via (i) electrostriction and (ii) the piezoelectric property of the medium; the presence of the finite amplitude pump wave is obviously the precondition for such a coupling and the consequent instability. The coupling has already been discussed earlier in connection with the general configuration. Equation (5.3) is now analyzed to obtain the expressions for (a) the threshold electric field required for the onset of instability and (b) the growth rate of the unstable mode well above the threshold. Separating the real and imaginary parts in Eq. (5.3) and solving for ω_i, we get

$$|\omega_i|_V=\frac{kv_{0x}e_{14}e'_{14}\omega_p^2|\omega_c|X}{4c_1^2\rho\epsilon|(\omega_0^2-\omega_c^2)|\left[1+\frac{\omega_p^2}{|\omega_0^2-\omega_c^2|}+\frac{kv_{0x}X}{2\omega_0}\right]kc_t} \ . \qquad (5.4)$$

The subscript V stands for the parameters under Voigt configuration. From the above expression, one can notice that the finite growth is achievable only when the magnetostatic field is present. As long as the factor $kv_{0x}X/2\omega_0$ (in the denominator) remains less than one corresponding to a value of $E_0\sim 10^7$ to 10^8 V m^{-1} and $|\omega_c|\sim 1.5\times 10^{14}$ sec^{-1}, the value of $|\omega_i|$ is found to be $\sim 8.91\times 10^4$ sec^{-1} which is smaller than that obtained under the general configuration ($\sim 10^6$ sec^{-1}).

B. Faraday geometry ($k_z\neq 0$, $k_x=0$)

Under this geometry, the dispersion relation is given by $a_{33}=0$ in Eq. (5.1) yielding

$$(\omega^2-k^2c_t^2)\left[\omega_1+\frac{i\omega_p^2}{\omega_s}\right]=\frac{\mu_0\gamma\omega_1e'_{14}k^2c_1^2E_0}{\rho} \ . \qquad (5.5)$$

It can be observed from this equation that the two modes are coupled via electrostriction only. However, the strong coupling at moderate electric field amplitude of the pump is achievable only in piezoelectric semiconductors remembering that $e'_{14}=e_{14}-\gamma E_0/2$ and $e_{14}>>\gamma E_0/2$ even for a very large value of E_0. The expression for the growth rate is found from Eq. (5.5) as

$$|\omega_i|_F=\frac{\mu_0\gamma\omega_0 e'_{14}k^2c_1^2E_0}{2\rho k c_t\omega_p^2}\ , \qquad (5.6)$$

where the suffix F stands for Faraday geometry.

The above equation indicates that the threshold value of E_0 is zero. Quite interestingly, one can notice from Eq. (5.5) that the magnetic field has no effect on the dispersion relation. Thus, the results will be similar to those obtained in Sec. III (with $k_x=0$). The numerical analysis made for n-InSb yields $|\omega_i|_F\sim 7.43\times 10^{-5}E_0$. This leads to the conclusion that under Faraday configuration, practically, Brillouin instability with significant growth is not achievable.

VI. CONCLUSIONS

The analytical investigations of Brillouin instability under various geometrical configurations of the electric field, magnetostatic field, and the wave vectors of the scattered modes have been dealt with in the present paper and one can arrive at the following conclusions: (1) From the comparison of results in Sec. III, IV, and V, we conclude that the magnetostatic field plays a very significant role. Brillouin instability with a significant growth of the unstable mode can be observable only in the magnetized piezoelectric semiconductor plasmas. Under Faraday geometry (Sec. V B), the terms arising due to magnetostatic field disappear and consequently, instability with almost no growth of the Brillouin mode can be observed, which is also the case with an isotropic plasma (Sec. III). (2) Under the general configuration, one can achieve a very large growth of the unstable mode which propagates with a phase velocity equal to the transverse acoustic velocity in the crystal. In order to get the best result, one must have to choose an appropriate value of θ for a certain value of the pump amplitude as well as the magnetic field. The role of magnetic field is to enhance the growth as well as to reduce the value of $E_{\rm cr}$. It must be noted that for low values of E_0 ($E_0<10^5$ V m^{-1}), the growth rate obtained by using Eq. (4.3) is $\sim 10^3$ sec^{-1}. (3) For the n-type cubic piezoelectric semiconductors under Voigt geometry, we find better growth of the unstable mode than under Faraday geometry. But the best geometry is found to be the general one with $0°<\theta<90°$. (4) The electric field amplitude E_0 considered in the present investigation can be expressed in terms of the pump intensity I_0 by using the relation $I_0=c_0\epsilon_0\epsilon_1|E_0|^2/2\eta$, η being the refractive index of the crystal ($=3.9$ for InSb) and c_0 is the velocity of light in vacuum. The results reported in this paper are made for E_0 in the range of 10^6 to 1.5×10^7 V m^{-1}; the corresponding range of I_0 using the above relation becomes 6.06×10^9 to 1.36×10^{12} W m^{-2}, which can be used without causing appreciable damage to the crystal.

ACKNOWLEDGMENTS

The authors are grateful to Professor P. G. Harper and Dr. S. Guha for encouragement. The financial support from the Science Research Council (U.K.) and Council of Scientific and Industrial Research (India) is also gratefully acknowledged.

[1]A. Yariv, in *Quantum Electronics,* 2nd ed. (Wiley, New York, 1975), p. 491.
[2]N. M. Kroll, J. Appl. Phys. 36, 34 (1965).
[3]C. L. Tang, J. Appl. Phys. 37, 2945 (1966).
[4]V. S. Starunov and I. L. Fabelinskii, Usp. Fiz. Nauk. 98, 441, (1969) [Sov. Phys.—Usp. 12, 463 (1970)].
[5]I. L. Fabelinskii, in *Quantum Electronics,* edited by H. Rabin and C. L. Tang (Academic, New York, 1975), Vol. I, Part A, pp. 363–418.
[6]P. K. Sen, Phys. Rev. B 21, 3604 (1980).
[7]P. Asam, W. Deuflhard, and W. Kaiser, Phys. Lett. 27A, 78 (1968).
[8]G. W. Winterling, W. Heiniche, and K. Dransfeld, in *Light Scattering Spectra in Solids,* edited by G. B. Wright (Springer, New York, 1969), pp. 489–591.
[9]R. S. Sussman and B. K. Ridley, J. Phys. C 7, 3941 (1974).
[10]H. E. Huey, A. Mase, and N. C. Luhmann, Jr., Phys. Rev. Lett. 45, 795 (1980).
[11]K. Nishikawa, J. Phys. Soc. Jpn. 24, 916 (1968); 24, 1152 (1968).
[12]R. B. Thompson and C. F. Quate, J. Appl. Phys. 42, 907 (1971).
[13]S. Guha and P. K. Sen, J. Appl. Phys. 50, 5387 (1979).
[14]G. M. Genkin, Fiz. Tekh. Poluprovod. 8, 1642 (1974) [Sov. Phys.—Semicond. 8, 1066 (1975)].
[15]J. F. Nye, in *Physical Properties of Crystals* (Clarendon, Oxford, 1957).
[16]D. A. Berlincourt, D. R. Curran, and H. Jaffe, in *Physical Acoustics, Principles and Methods,* edited by W.

P. Mason (Academic, New York, 1964), Vol. I, Part A, pp. 169–270.
[17]J. W. Tucker and V. W. Rampton, in *Microwave Ultrasonics in Solid State Physics* (North-Holland, Amsterdam, 1972), p. 20.
[18]W. Hayes and R. Loudon, in *Scattering of Light by Crystals* (Wiley, New York, 1978), pp. 332–340.
[19]S. Guha and P. K. Sen, Indian J. Phys. 53B, 228 (1979).